New Observations of Stratospheric N_2O_5

C. P. Rinsland
Atmospheric Sciences Division
NASA Langley Research Center
Hampton, VA

G. C. Toon, C. B. Farmer, and R. H. Norton
Jet Propulsion Laboratory
California Institute of Technology
Pasadena, CA

J. S. Namkung
ST Systems Corporation
Hampton, VA

Abstract

The unequivocal detection of N_2O_5 in the stratosphere was reported by Toon et al. (1986, 1987) based on measurements of the absorption by the N_2O_5 bands at 1246 and 1720 cm^{-1} in solar occultation spectra recorded at sunrise near 47°S latitude by the Atmospheric Trace Molecule Spectroscopy (ATMOS) experiment during the Spacelab 3 (SL3) shuttle mission (April 29-May 6, 1985). In this work, we report additional measurements and analysis of stratospheric N_2O_5 derived from the ATMOS/SL3 spectra. The primary results are the detection and measurement of N_2O_5 absorption at sunset in the lower stratosphere, the inversion of a precise (~10%) N_2O_5 sunrise vertical distribution between 25.5- and 37.5-km altitude, and the identification and measurement of absorption by the N_2O_5 743-cm^{-1} band at sunrise. Assuming 4.32×10^{-17} and 4.36×10^{-17} cm^{-1}/molecule cm^{-2} respectively for the integrated intensities of the 1246- and 743-cm^{-1} bands at stratospheric temperatures, retrieved volume mixing ratios in parts per billion by volume (ppbv) at sunrise (47°S latitude) are 1.32 ± 0.34 at 37.5 km, 1.53 ± 0.35 at 35.5 km, 1.63 ± 0.36 at 33.5 km, 1.60 ± 0.34 at 31.5 km, 1.43 ± 0.30 at 29.5 km, 1.15 ± 0.24 at 27.5 km, and 0.73 ± 0.15 at 25.5 km. Retrieved VMRs in ppbv at sunset (30°N latitude) are 0.13 ± 0.05 at 29.5 km, 0.14 ± 0.05 at 27.5 km, and 0.10 ± 0.04 at 25.5 km. Quoted error limits (1 sigma) include the error in the assumed band intensities (~20%). Within the error limits of the measurements, the inferred mixing ratios at sunrise agree with diurnal photochemical model predictions obtained by two groups using current photochemical data. The measured mixing ratios at sunset are lower than the model predictions with differences of about a factor of 2 at 25-km altitude.

1. Introduction

Nitrogen pentoxide (N_2O_5) is an important temporary reservoir of stratospheric odd nitrogen, which can destroy ozone through catalytic reactions involving NO and NO_2 [Crutzen, 1970]. N_2O_5 is produced at night by a three body reaction of NO and NO_2. During daytime N_2O_5 is slowly destroyed with a time scale on the order of hours to days below 40 km [Brasseur et al., 1987].

Following two tentative observations [Roscoe, 1982; Evans, 1986], N_2O_5 was identified unambiguously through simultaneous sunrise measurements of the broad, unresolved absorption envelopes of two N_2O_5 features, the ν_{12} band in the 1230 to 1260 cm^{-1} region and the overlapping ν_1 and ν_{11} bands in the 1680 to 1760 cm^{-1} region [Toon et al., 1986; Toon, 1987]. These features were detected in 0.015-cm^{-1} resolution (apodized) solar occultation spectra recorded from orbit by the Atmospheric Trace Molecule Spectroscopy (ATMOS) Fourier transform spectrometer during the Spacelab 3 (SL3) shuttle mission (April 29-May 6, 1986). The ATMOS measurements, obtained at sunrise and sunset, indicated strong diurnal variation of stratospheric N_2O_5. Subsequent midnight to predawn spectroscopic observations obtained in emission at an apodized resolution of 0.044 cm^{-1} also showed the ν_{12} band of N_2O_5 [Kunde et al., 1988].

In the present study, we report further analysis of the ATMOS/SL3 spectra to obtain quantitative information on stratospheric N_2O_5. The most important new result is the detection of weak absorption by the N_2O_5 ν_{12} band at sunset in the lower stratosphere, confirming model predictions that not all of this molecule is photodissociated during the day except in polar regions during the extended daylight of summer (see, for example, Herman [1979], Fabian et al. [1982], and Brasseur et al. [1987]). In addition, we have derived refined measurements of

the absorption by the N_2O_5 ν_{12} band at sunrise. These measurements have been used to invert a precise vertical profile distribution between 25.5 and 37.5 km altitude. We also report the identification of the broad, unresolved envelope of another N_2O_5 feature, the overlapping ν_3 and ν_{14} bands centered at 743 cm^{-1} [Hisatsune et al., 1962], in a series of stratospheric spectra recorded at sunrise.

2. Experimental

The ATMOS instrument consists basically of a fast scanning double-passed Michelson' interferometer, a suntracker and telescope, and a HgCdTe detector cooled to 77 K by a split Stirling-cycle cooler. Spectral coverage was defined prior to each occultation by selecting in real time one of four overlapping broadband interference filters covering altogether 600 to 4800 cm^{-1}. A "notch" filter was used during a single sunrise occultation to record spectra of the 600 to 750 cm^{-1} and 2000 to 2500 cm^{-1} regions. Every 2.2 seconds, a two-sided, 800,000-point solar interferogram with a maximum path difference of 47.5 cm was recorded, yielding spectra with an unapodized resolution of 0.01 cm^{-1}. From the Spacelab 3 orbital altitude of ~360 km, this spacing in time corresponded to successive tangent height differences of ~4.1 km in the upper atmosphere. This spacing was reduced in the lower stratosphere and troposphere by the drift of the suntracker field of view toward the upper limb of the "flattened" solar disk at high zenith angles. ATMOS spectra were recorded during 19 occultations, 12 sunsets between 25.6°N and 32.7°N latitude and 7 sunrises between 46.7°S and 49.0°S latitude, from April 29 to May 1, 1985. Additional details of the instrument and its operation during the Spacelab 3 mission have been described by Farmer and Raper [1986] and Farmer et al. [1987].

ATMOS spectra are derived from the inverse Fourier transform of two-sided interferograms with the same central fringe measurement. The intensities at each wavenumber in the low sun (atmospheric) spectra are subsequently ratioed to a corresponding value in a high sun (exo-atmospheric) spectrum to eliminate solar features and to remove the wavelength dependence of the instrumental response and the solar flux. Additional details of the processing of the ATMOS data and the spectral analysis software will be described in a future publication (R. H. Norton, unpublished results, 1989).

In the present analysis, we used the Spacelab 3 spectra recorded with filter 1 (600 to 1200 cm^{-1}) and filter 2 (1100 to 2000 cm^{-1}). Table 1 gives measurement parameters for each of the occultations. Because of the weakness of the N_2O_5 absorption at sunset, spectra recorded at approximately equal tangent heights from three sunset (SS) occultations (SS02, SS05, and SS08 for filter 1; SS03, SS07, and SS12 for filter 2) were coadded to obtain sets of zonal average sunset spectra with improved signal-to-noise ratios of ~400 in filter 1 and ~300 in filter 2.

Pressures and temperatures assumed in the analysis were derived from the ATMOS filter 3 spectra (1580-3400 cm^{-1} region) by analyzing isolated absorption lines of gases with well-known atmospheric volume mixing ratios (CO_2 and N_2). The temperature versus pressure distributions retrieved from the four filter 3 sunset occultations were found to be very similar, and, for this reason, they were combined to obtain a zonal average pressure-temperature distribution for ~28°N latitude. The same averaging procedure could not be followed for ~47°S latitude because only a single filter 3 sunrise (SR) occultation, SR02, was recorded in the southern hemisphere. The northern hemisphere zonal average or the single southern hemisphere pressure versus temperature distribution from

filter 3 was adopted, as appropriate, in the analysis of the filter 1 and 2 spectra since only less favorable lines were available for retrievals in these spectral regions. Assuming these distributions, tangent pressures of the individual filter 1 and 2 spectra were then determined by either spectral fitting isolated CO_2 lines with temperature-insensitive intensities or extrapolating altitude spacings based on the mission ephemeris. Additional details of the pressure-temperature analysis are described by Rinsland et al. [1987] and Gunson et al. [1989].

3. Analysis

Laboratory spectra recorded at 0.02 cm^{-1} resolution [Murcray et al., 1984] show that both the 1246-cm^{-1} and 1720-cm^{-1} N_2O_5 bands appear as broad, unresolved features at the resolution of the ATMOS instrument, with no evidence for fine structure. Similarly, unpublished 0.005-cm^{-1} resolution laboratory spectra of the 743 cm^{-1} N_2O_5 band recorded at Kitt Peak also show no fine structure (E. Cohen, Jet Propulsion Laboratory, private communication, 1989). In stratospheric spectra, each of the broad N_2O_5 features is superimposed on the absorption by a large number of lines produced by molecules such as CH_4, N_2O, CO_2, and HNO_3 (see Toon et al. [1986], Figure 1; Toon [1987], Figures 1 and 2; Kunde et al. [1988], Figures 1 and 2). Because of high spectral resolution of the ATMOS data, it is possible to locate microwindows where interfering line absorption is small so that direct measurements of the N_2O_5 absorption can be obtained.

Measurements of the broad envelopes of the N_2O_5 absorption features have been derived following the procedures described in a recent study of stratospheric infrared continuous absorptions using the ATMOS/Spacelab 3 spectra [Rinsland et al., 1988]. Microwindows, ~0.02 cm^{-1} wide, where interfering atmospheric line

absorption is minimal were chosen every ~1 cm^{-1} across the entire extent of the N$_2$O$_5$ features based on synthetic spectrum calculations generated using the ATMOS line list [Brown et al., 1987] and volume mixing ratio profiles retrieved from the ATMOS spectra [e.g. Gunson et al., 1989]. Measurements were included only if interfering line absorption was calculated to be less than ~3% in the microwindow. This limit restricted the analysis to tangent heights above 23 km for the 1246-cm^{-1} band. Interfering line absorption is much stronger in the region of the 743-cm^{-1} band so that measurements in this region were limited to tangent heights above 29 km. The ATMOS spectra were also examined to verify that each of the microwindows is free of unidentified lines.

Table 2 presents a listing of the wavenumber limits of each of microwindows used in this study. Microwindows designated "x" are in regions containing significant N$_2$O$_5$ absorption. Microwindows marked "t" are outside of the N$_2$O$_5$ absorption regions and were used to determine the 100% transmittance levels in each spectrum as described below.

The intensities $I_{\nu,m}$ measured from an ATMOS spectrum at a microwindow located at wavenumber ν were first corrected for interfering line absorption using the expression

$$I_{\nu,c} = I_{\nu,m}/T_{\nu,i} \qquad (1)$$

where $T_{\nu,i}$ is the calculated transmittance due to interfering atmospheric lines, $I_{\nu,c}$ is the corrected intensity, and ν is the wavenumber (cm^{-1}). Error bars on $I_{\nu,c}$ are 1 to 2% based on the spectral signal-to-noise ratio (~0.5% of $I_{\nu,m}$), the uncertainty in the correction for interfering line absorption (± 20%), and the uncertainty in the 0% transmission level in the spectrum (± 0.5% of $I_{\nu,m}$). The intensity levels $I_{\nu,t}$ corresponding to the 100% transmittance levels in the

spectra were derived by least-squares fitting the $I_{\nu,c}$ values from the "t" microwindows using the expression

$$I_{\nu,t} = a + b(\nu - \nu_r) \tag{2}$$

where a and b are fitted coefficients determined for each spectrum and ν_r is an arbitrary reference wavenumber. From Eq. 2 and the fitted coefficients, the transmittance due to N_2O_5 absorption $T_{\nu,n}$ was calculated at the wavenumber of each microwindow from

$$T_{\nu,n} = I_{\nu,c}/I_{\nu,t} \tag{3}$$

and the equivalent width W of the N_2O_5 feature was computed from

$$W = \int (1 - T_{\nu,n}) \, d\nu \qquad \cdot \tag{4}$$

with integration limits of 1226 and 1265 cm^{-1} for the ν_{12} band and 725 and 760 cm^{-1} for the overlapping ν_3 and ν_{14} bands. The regions used to fit the 100% transmittance level were 1210 to 1226 cm^{-1} and 1265 to 1270 cm^{-1} for the ν_{12} band and 716 to 725 cm^{-1} and 760 to 770 cm^{-1} for the overlapping ν_3 and ν_{14} bands.

3.1 $1246\text{-}cm^{-1}$ (ν_{12}) Feature

Figure 1 shows examples of measurements obtained for the 1246 cm^{-1} band at sunrise from occultation SR05. The uppermost spectrum (tangent height of 41.9 km corresponding to a tangent pressure of 1.9 mbar) shows no obvious absorption by N_2O_5. The measured equivalent width is 0.03 ± 0.04 cm^{-1} (1 sigma). The next lower spectrum in the figure (tangent height of 33.8 km corresponding to a tangent pressure of 6.4 mbar) shows detectable absorption by N_2O_5 (equivalent width of 0.59 ± 0.04 cm^{-1}). The absorption is much stronger in the third and fourth spectra (tangent heights of 26.9 and 24.0 km corresponding respectively to tangent pressures of 18.6 and 29.4 mbar). Comparison of the later two curves with the calculated spectrum of N_2O_5 obtained from the room temperature cross

sections of Massie et al. [1985] (bottom curve) shows good agreement between the measured and calculated N_2O_5 band shapes (except for a minor difference discussed below). The contours of the P, Q, and R branches of the N_2O_5 band are clearly visible in the lower altitude measurements. Note that the total absorption is nearly equal for the 26.9 and 24.0 km scans (equivalent widths of 1.66 ± 0.06 and 1.75 ± 0.06 cm^{-1}, respectively), despite a factor of 1.60 between the airmasses of the two scans, indicating that the volume mixing ratio of N_2O_5 is declining rapidly with decreasing altitude between 26.9 and 24.0 km.

When the measured and calculated curves are overlayed (e.g. Figure 2), the N_2O_5 feature is slightly narrower in the stratospheric spectra than in the calculated spectra for 296 K. This change is in agreement with changes in band contours measured in the laboratory between room and stratospheric temperatures for several heavy molecules (e.g. $ClONO_2$ [Ballard et al., 1988], CF_2Cl_2 [Elkins and Sams, 1986; Nguyen-Van-Thanh et al., 1986], and $CFCl_3$ [Nanes et al. 1980; Elkins and Sams, 1986]). Cantrell et al. [1988] reported that their laboratory measurements show no significant changes in the integrated absorption and peak height of the 1246-cm^{-1} N_2O_5 band between 233 and 350 K. Unfortunately, the variation of the shape of the band with temperature was not discussed.

Figure 3 presents a plot of the measured equivalent widths of the N_2O_5 1246-cm^{-1} band as a function of tangent height derived from the sunrise occultation SR05 and filter 2 zonal average spectra. Measured equivalent widths more than 3 times the estimated 1-sigma error limit (± 0.04 cm^{-1} above 28 km, ± 0.06 cm^{-1} below 28 km for SR05; ± 0.026 cm^{-1} above 28 km, ± 0.04 cm^{-1} below 28 km for the zonal average spectra) are obtained from five SR05 spectra with tangent heights between 37.6 and 24.0 km and three sunset spectra with tangent heights of 29.6, 26.0, and 23.0 km (tangent pressures of 12.8, 21.8, and 34.6 mbar, respectively).

To illustrate the N_2O_5 absorption measured in the sunset spectra, the 26.0 km tangent height sunset measurements are plotted in Figure 4 along with the SR05 data for a tangent height of 37.6 km. The sunrise spectrum was included because the strength of the N_2O_5 absorption is nearly equal to that in the sunset spectrum. Despite the weakness of the absorption (maximum optical depth ~1%), there is good agreement between the measured location and shape of the N_2O_5 features in the two spectra, adding confidence to the identification of N_2O_5 absorption in the sunset spectra.

Because of the good quality and wide range of altitudes of the SR05 measurements, it was possible to invert the sunrise profile directly from the measured equivalent widths. For this purpose, we used the onion-peeling retrieval technique and assumed linear absorption by N_2O_5 and an integrated band intensity of 4.32×10^{-17} cm^{-1}/molecule cm^{-2} at all temperatures. The assumption of linear absorption by N_2O_5 should be accurate to better than 1% since the N_2O_5 optical depth does not exceed 10% in any of the spectra. The value assumed for the 1246 cm^{-1} band integrated intensity was adopted from the analysis of the ATMOS observations by Toon et al. [1986]. It has been chosen for consistency with the latter study and also because it agrees fairly well with most of the reported measurements (see Table 1 of Cantrell et al. [1988] for a summary of the published laboratory measurements of N_2O_5 integrated band intensities and peak absorption cross sections). Exceptions are integrated intensities of 2.36 $\times$ 10^{-17} cm^{-1}/molecule cm^{-2} at 298 K [Lovejoy et al., 1980] and 5.11 $\times$ 10^{-17} cm^{-1}/molecule cm^{-2} at 298 K [Camy-Peyret et al., 1988] (a revision of the results from an earlier study [Camy-Peyret et al., 1987]). Only the data of Cantrell et al. [1988] cover the range of stratospheric temperatures; all other values were derived from spectra of N_2O_5 samples at room temperature. Based on the

agreement between the reported measurements, an uncertainty of 20% for the 1246 cm^{-1} integrated band intensity has been adopted in our error budget calculations. This error estimate has been revised downward from the value of 50% reported previously [Russell et al., 1988].

The relatively wide tangent height spacings between successive ATMOS spectra (2.9 to 4.1 km) required that we include a number of additional layers in the model atmosphere between the altitudes defined by the tangent heights of the spectra. Layer thicknesses of ~0.5 km were used. In the analysis of the equivalent width from each scan, the volume mixing ratio (VMR) values in all layers with boundary altitudes between the tangent heights of the scan and the previous scan were scaled by a multiplicative factor to obtain equal measured and calculated equivalent widths. Initially, a constant N_2O_5 volume mixing ratio in the stratosphere was assumed. However, this distribution is not realistic, and a "saw-tooth" vertical profile was obtained with VMR discontinuities at the altitudes corresponding to the tangent heights of the spectra. These discontinuities were removed by smoothing the vertical profile by fitting the measurements with a cubic function to describe the variation of the VMR with altitude. The analysis and smoothing were repeated several times until a continuous vertical VMR distribution was retrieved at all altitudes. Although the smoothing function is somewhat arbitrary, tests with different, realistic smoothing expressions indicate that this procedure is unlikely to result in errors of more than 5% in the relative vertical distribution.

Because N_2O_5 absorption is much weaker in the sunset spectra, the vertical profile can only be retrieved below an altitude of ~30 km. To obtain a realistic profile shape above 30 km, we scaled a N_2O_5 vertical profile calculated for sunset with a diurnal photochemical model by a mutiplicative factor until equal

measured and calculated equivalent widths were obtained for the 29.6-km tangent height spectrum. The model calculations (M. Natarajan, private communication, 1989) were computed for the same latitude and date as the ATMOS measurements and assume at each altitude the appropriate ATMOS pressures and temperatures and the measured mixing ratios of O_3, CH_4, and H_2O [Gunson et al., 1989], total odd nitrogen [Russell et al., 1988], and total odd chlorine [Raper et al., 1987]. The retrieval analysis for the lower altitudes followed that described for the sunrise spectra.

In Tables 3 and 4, the retrieved VMR values along with estimated precisions and absolute error limits (1 sigma) are given at altitude spacings of 2 km. Precisions have been estimated from the accuracy of the equivalent width measurements, the uncertainty in the inversion technique, and the precision of the ATMOS tangent pressures and corresponding tangent heights. The absolute errors at each altitude include the estimated uncertainty in the assumed N_2O_5 integrated band intensity and the systematic errors in the tangent pressures and corresponding tangent heights. See Gunson et al. [1989] for a detailed discussion of the ATMOS/SL3 error budget.

3.2 743-cm^{-1} (ν_3, ν_{14}) Feature

Although the 743-cm^{-1} band of N_2O_5 is about as strong as the 1246 cm^{-1} band [Lovejoy et al., 1980; Cantrell et al., 1988], the spectral region containing the 743-cm^{-1} band is much less favorable for quantitative measurements because of strong interference by atmospheric lines, primarily due to O_3 and CO_2. Nevertheless, at high altitudes (above ~29 km), it is possible to observe the broad absorption envelope of the 743 cm^{-1} band in spectra from ATMOS occultation SR06, the only sunrise event recorded with filter 1 (600-1200 cm^{-1}).

In Figure 5, spectra recorded at sunrise and sunset near a tangent height of 32 km are plotted on an expanded vertical scale over the region of the 743-cm^{-1} N_2O_5 band. A broad absorption envelope covering 725 to 760 cm^{-1} is superimposed on the line absorption in the sunrise spectrum, but this broad envelope is not apparent in the sunset spectrum. To confirm that the broad feature results from N_2O_5 absorption, the transmittance due to N_2O_5 alone was calculated using the cross sections at 273 K reported in Figure 1 of Cantrell et al. [1988]. The transmittance curve obtained for a N_2O_5 column amount of 2.0 $\times$ 10^{16} molecules cm^{-2} is plotted with the sunrise spectrum and shows that the difference between the sunrise and sunset absorption can be explained by enhanced absorption by N_2O_5 in the sunrise spectrum. Similar results are obtained from comparisons of sunrise-sunset sets of spectra recorded near 36 and 29 km. At lower altitudes, the sunrise-sunset difference is less apparent because of the intense, overlapping absorption by atmospheric lines.

Although less satisfactory for quantitative analysis, it is nevertheless useful to compare retrievals from the 743-cm^{-1} feature with those from the 1246-cm^{-1} feature to test the consistency of the results and to provide further confirmation of the identification of the 743-cm^{-1} feature. We therefore selected the microwindows listed in Table 2 and obtained the sequence of sunrise measurements shown in Figure 6. The envelope of the N_2O_5 band is not apparent in the measurements (at top) for a tangent height of 41.4 km (tangent pressure of 2.1 mbar), but can be seen in the measurements (next two lower curves) for tangent heights of 33.3 and 29.8 km (tangent pressures of 6.9 and 11.8 mbar, respectively). The bottom curve shows the calculation of the N_2O_5 absorption obtained with the Cantrell et al. [1988, Figure 1] cross sections at 273 K and a N_2O_5 column amount of 4.0 $\times$ 10^{16} molecules cm^{-2}.

Because of the strong interference, it was not possible to identify absorption by the 743-cm^{-1} N_2O_5 feature in the filter 1 sunset spectra. A weak, unidentified absorption feature was observed in the 725- to 735-cm^{-1} interval of the zonal average sunset spectra with tangent heights of 36.8, 32.7, and 28.9 km (tangent pressures of 4.6, 8.2, and 14.2 mbar, respectively). Although this absorption overlaps the contour of the 743-cm^{-1} N_2O_5 feature, the unidentified feature is offset to lower wavenumber, and therefore is produced mostly by some other molecule. Measured equivalent widths and estimated 1-sigma error limits (in cm^{-1}) are 0.08 ± 0.03 at 36.8 km, 0.12 ± 0.05 at 32.7 km, and 0.20 ± 0.08 at 28.9 cm^{-1}. The location of the unassigned absorption occurs in the region containing the strongest R branch lines of the intense 10001←01101 band of $^{12}C^{16}O_2$. It is possible that our corrections underestimate the residual absorption by the wings of these lines. We have assumed that the unassigned absorption is also present in the sunrise data and have corrected the measured N_2O_5 equivalent widths based on the sunset results.

The integrated ν_3/ν_{14} band intensity of 4.36×10^{-17} cm^{-1}/molecule cm^{-2} reported by Cantrell et al. [1988] was adopted in the analysis of the equivalent widths derived from the sunrise spectra. Because of the increased uncertainty in the equivalent widths due to interference effects, the shape of the vertical distribution was poorly determined using the onion-peeling retrieval technique. We therefore derived the VMR profile by scaling the vertical distribution retrieved from the filter 2 sunrise measurements (1246-cm^{-1} band) until the sum of the squares of the measured equivalent widths was minimized. The resulting scaling factor 1.02 ± 0.15 indicates consistency between the results for the two bands, although the error limit is rather large. The scaled profile is included in Table 3, although the estimated precisions are considerably poorer

than derived for the 1246-cm^{-1} band. The absolute accuracies have been derived assuming an uncertainty of 20% for the adopted 743-cm^{-1} integrated band intensity. The SR06 measurements have little impact on the weighted average volume mixing ratios at sunrise reported in Table 3.

4. Discussion

In Figure 7, the present results, previous measurements, and photochemical model calculations are plotted as a function of altitude. The preliminary sunrise profile derived by Toon et al. [1986] was obtained from analysis of the 1246-cm^{-1} band in the ATMOS SR05 spectra using a different approach than adopted in the present study. In the earlier work, the N_2O_5 profile was obtained by scaling a reference photochemical model profile by a single multiplicative factor until the N_2O_5 envelopes in synthetic spectra matched those in the measured spectra [Toon et al., 1986; Russell et al., 1988]. Hence, the sunrise vertical distribution was assumed, not retrieved, as in the present investigation (recall that both studies have assumed the same value for the integrated intensity of the 1246-cm^{-1} band). Above 33 km, the two profiles agree within 15%, with the present profile the lower of the two above 34 km. Below 33 km, our revised volume mixing ratios are higher with the maximum difference in percent occurring at 27.5 km where we obtain 1.15 ppbv as compared to 0.77 ppbv previously. The N_2O_5 predawn profile derived from emission measurements of the 1246 cm^{-1} band [Kunde et al., 1988] is slightly higher than the ATMOS sunrise profile, in general accordance with diurnal changes predicted by photochemical models.

The diurnal photochemical model profiles plotted in Figure 7 (M. Natarajan, private communication, 1989; M. Allen, private communication, 1989) were computed with the chemical kinetic and photochemical data from the recent NASA evaluation

[NASA-JPL, 1987]. The model calculations are described elsewhere [Natarajan and Callis, 1989; M. Allen, manuscript in preparation, 1989]. Within the measurement error limits, the sunrise observations and the profiles predicted with the two models agree at all altitudes. The agreement between measurement and calculation is less satisfactory at sunset with both diurnal photochemical models predicting higher VMRs than the ATMOS measurements. Although the measurement error limits are large, there is also an indication that the maximum N_2O_5 VMR at sunset occurs at a slightly higher altitude in the measurements (~28 km) than in the calculations (~26 km). Based on the present measurements and the sum of total odd nitrogen derived from the ATMOS profiles [Russell et al., 1988], the contribution of N_2O_5 at sunset is negligible, at most only ~2% of the total with the maximum at 27 km.

In a recent review, Brasseur et al. [1987] emphasized that calculations of the nitrogen oxides in the stratosphere are sensitive to a number of effects. For example, multiple scattering by molecules and aerosols, the aerosol load of the atmosphere, and the albedo are important in determining the N_2O_5 photodissociation rate, especially at high solar zenith angles. The accuracy in calculating the photodissociation rate is also limited by the uncertainties in the recommended absorption cross sections and their temperature dependences. The combined uncertainty in the cross sections and the quantum yields for N_2O_5 photodissociation, taking into account the atmospherically important wavelength regions, is rather large, about 2.0 [NASA/JPL, 1987, Table 5]. A combination of these effects is likely to be responsible for the difference between the observations and model results at sunset.

5. Conclusions

In this paper we have reported the analysis of two infrared absorption features of N_2O_5 observed in the ATMOS/SL3 spectra of the stratosphere. The primary results are the detection and quantitative measurement of absorption by the 1246-cm^{-1} band at sunset in the lower stratosphere and the retrieval of a precise (~10%) sunrise vertical distribution covering the 25.5- to 37.5-km altitude region. Including systematic error effects, the 1-sigma error bars of the retrieved volume mixing ratios vary from ± 21% at 25.5 km to ± 26% at 37.5 km for the sunrise measurements and are ± 38% for the sunset results at 25.5 km. The uncertainty in the N_2O_5 integrated band intensities at stratospheric temperatures (± 20% has been assumed for both the 743- and 1246-cm^{-1} features) contributes significantly to the absolute uncertainties. Within the error limits, the retrieved N_2O_5 sunrise volume mixing ratios agree at all altitudes with profiles calculated with two different diurnal photochemical models, but the measured sunset values are about a factor of two lower than values calculated with the same models. Also, in this work, the detections of the 1246- and 1720-cm^{-1} N_2O_5 features [Toon et al., 1986; Toon, 1987] have been extended by the identification of the 743-cm^{-1} N_2O_5 feature (overlapping ν_3 and ν_{14} bands) in the ATMOS filter 1 sunrise spectra. Strong spectral interference in the region of the 743-cm^{-1} feature limits the accuracy of the measurements and the altitude coverage to tangent heights above ~29 km. Within the error limits, the sunrise profiles deduced from the 743- and 1246-cm^{-1} features are consistent. The 743-cm^{-1} band was not detected in the spectra recorded at sunset due to the strong interference in the lower stratospheric scans.

Flights of the ATMOS instrument over the upcoming decade will cover a wide variety of geographic locations during different seasons, including the high

latitude sunlit boundary of the polar night where high concentrations of N_2O_5 are expected. The resulting simultaneous measurements of N_2O_5 and the other main constituents of the $[NO_y]$ chemical family along with measurements of other key stratospheric species will provide important observational data for additional testing of photochemical model predictions.

Acknowledgments

References

Ballard, J., W. B. Johnston, M. R. Gunson, and P. T. Wassell, Absolute absorption coefficients of $ClONO_2$ infrared bands at stratospheric temperatures, J. Geophys. Res., 93, 1659-1665, 1988.

Brasseur, G., D. Cariolle, A. De Rudder, L. J. Gray, J. A. Pyle, E.-P. Röth, U. Schmailzl, and D. J. Wuebbles, Odd nitrogen during the MAP/GLOBUS 1983 campaign: Theoretical considerations, Planet. Space Sci., 35, 637-645, 1987.

Brown, L. R., C. B. Farmer, C. P. Rinsland, and R. A. Toth, Molecular line parameters for the atmospheric trace molecule spectroscopy experiment, Appl. Opt., 26, 5154-5182, 1987.

Camy-Peyret, C., J.-M. Flaud, L. Lechuga-Fossat, G. Laverdet, and G. Le Bras, The absorption of gaseous dinitrogen pentoxide in the 8.1 and 5.7 μm spectral regions, Chem. Phys. Lett., 139, 345-349, 1987.

Camy-Peyret, C., J.-M. Flaud, L. Lechuga-Fossat, G. Laverdet, and G. Le Bras, Erratum: The absorption of gaseous dinitrogen pentoxide in the 8.1 and 5.7 μm spectral regions, Chem. Phys. Lett., 148, 364, 1988.

Cantrell, C. A., J. A. Davidson, A. H. McDaniel, R. E. Shetter, and J. G. Calvert, Infrared absorption cross sections for N_2O_5, Chem. Phys. Lett., 148, 358-363, 1988.

Crutzen, P. J., The influence of nitrogen oxides on atmospheric ozone content, Quart. J. R. Met. Soc., 96, 320-325, 1970.

Elkins, J. W., and R. L. Sams, Measurements of the temperature dependence on the infrared band strengths for halocarbons F-11 and F-12, Natl. Bur. Stand. U.S. Rep. 553-K-86, CMA Ref. Rep. FC83-473, 22 pp., 1986.

Evans, W. F. J., Observation of the 8-μm N_2O_5 thermal emission feature in the stratosphere, Appl. Opt., 25, 1866-1868, 1986.

Fabian, P., J. A. Pyle, and R. J. Wells, Diurnal variations of minor constituents in the stratosphere modeled as a function of latitude and season, J. Geophys. Res., 87, 4981-5000, 1982.

Farmer, C. B., and O. F. Raper, High resolution infrared spectroscopy from space: A preliminary report on the results of the Atmospheric Trace Molecule Spectroscopy (ATMOS) experiment on Spacelab 3, NASA Conference Proceedings, "Spacelab 3 Mission Review," NASA Conf. Proc., CP-2429, May 1986. (Available from the Natl. Tech. Inf. Serv., Springfield, Va.)

Farmer, C. B., O. F. Raper, and F. G. O'Callaghan, Final report on the first flight of the ATMOS instrument during the Spacelab 3 mission, April 29 through May 6, 1985, JPL Publ. 87-32, 45pp., Jet Propulsion Laboratory, Pasadena, California, Oct. 1, 1987.

Gunson, M. R., C. B. Farmer, R. H. Norton, R. Zander, C. P. Rinsland, J. Shaw, and B.-C. Gao, Measurements of CH_4, N_2O, CO, H_2O and O_3 in the middle atmosphere by the ATMOS experiment on Spacelab 3, submitted to J. Geophys. Res., 1989.

Herman, J. R., The problem of nighttime stratospheric NO_3, J. Geophys. Res., 84, 6336-6338, 1979.

Hisatsune, I. C., J. P. Devlin, and Y. Wada, Vibrational spectrum and structure of N_2O_5, Spectrochim. Acta, 18, 1641-1653, 1962.

Kunde, V. G., J. C. Brasunas, W. C. Maguire, J. R. Herman, S. T. Massie, M. M. Abbas, L. W. Herath, and W. A. Shaffer, Measurement of nighttime stratospheric N_2O_5 from infrared emission spectra, Geophys. Res. Lett., 15, 1177-1180, 1988.

Lovejoy, R. W., C. Chackerian, Jr., and R. W. Boese, Integrated band intensities of gaseous N_2O_5, Appl. Opt., 19, 744-748, 1980.

Massie, S. T., A. Goldman, D. G. Murcray, and J. C. Gille, Approximate absorption cross sections of F12, F11, $ClONO_2$, N_2O_5, HNO_3, CCl_4, CF_4, F21, F113, F114, and HNO_4, Appl. Opt., 24, 3426-3427, 1985.

Murcray, D. G., F. J. Murcray, A. Goldman, F. S. Bonomo, and R. D. Blatherwick, High resolution IR laboratory spectra, Appl. Opt., 23, 3502, 1984.

NASA-JPL, Chemical kinetics and photochemical data for use in stratospheric modeling, Evaluation No. 8, JPL Publication 87-41, 1987.

Nanes, R., P. M. Silvaggio, and R. W. Boese, Temperature dependence of intensities of the 8-12 μm bands of CFCℓ_3, <u>J. Quant. Spectrosc. Radiat. Transfer</u>, <u>23</u>, 211-220, 1980.

Natarajan, M., and L. B. Callis, Examination of stratospheric ozone photochemistry in light of recent data, <u>Geophys. Res. Lett.</u>, submitted, 1989.

Nguyen-Van-Thanh, I. Rossi, A. Jean-Louis, and H. Rippel, Infrared band shapes and band strengths of CF$_2$Cℓ_2 from 800 to 1200 cm^{-1} at 296 and 200 K, <u>J. Geophys. Res.</u>, <u>91</u>, 4056-4062, 1986.

Raper, O. F., C. B. Farmer, R. Zander, and J. H. Park, Infrared spectroscopic measurements of halogenated sink and reservoir gases in the stratosphere with the ATMOS instrument, <u>J. Geophys. Res.</u>, <u>92</u>, 9851-9858, 1987.

Rinsland, C. P., J. M. Russell III, J. H. Park, and J. Namkung, Retrieval of upper atmosphere pressure-temperature profiles from high resolution solar occultation spectra, NASA Tech. Memo. 89160, NASA Langley Res. Cent., Hampton, Va., 1987. (Available from the Natl. Tech. Inf. Serv., Springfield, Va.)

Rinsland, C. P., R. Zander, J. S. Namkung, C. B. Farmer, and R. H. Norton, Stratospheric infrared continuum absorptions observed by the ATMOS instrument, submitted to <u>J. Geophys. Res.</u>, 1988.

Roscoe, H. K., Tentative observation of stratospheric N_2O_5, <u>Geophys. Res. Lett.</u>, <u>9</u>, 901-902, 1982.

Russell, J. M. III, C. B. Farmer, C. P. Rinsland, R. Zander, L. Froidevaux, G. C. Toon, B. Gao, J. Shaw, and M. Gunson, Measurements of odd nitrogen compounds in the stratosphere by the ATMOS experiment on Spacelab 3, <u>J. Geophys. Res.</u>, <u>93</u>, 1718-1736, 1988.

Toon, G., Reply: Detection of stratospheric nitrogen species, <u>Nature</u>, <u>330</u>, 427, 1987.

Toon, G. C., C. B. Farmer, and R. H. Norton, Detection of stratospheric N_2O_5 by infrared remote sounding, <u>Nature</u>, <u>319</u>, 570-571, 1986.

TABLE 1. ATMOS/SL3 Occultations Analyzed in this Study

Filter No.	Occultation Name	Month/Day of 1985	Latitude (deg.)	Longitude (deg. West)
		Sunsets		
1	SS02	04/30	32.7 N	244.6
1	SS05	04/30	31.4 N	359.6
1	SS08	05/01	29.9 N	114.6
2	SS03	04/30	32.3 N	290.6
2	SS07	05/01	30.3 N	91.6
2	SS12	05/01	25.9 N	53.7
		Sunrises		
1	SR06	05/01	46.9 S	50.1
2	SR05	05/01	47.0 S	27.2

SS indicates sunset; SR, sunrise. Spectral coverage with filter 1, 600-1200 cm^{-1}, filter 2, 1100-2000 cm^{-1} (field of view 2 mrad with both filters corresponding to 4 km altitude at the horizon).

TABLE 2. Microwindow Regions (cm^{-1}) used in the Analysis

Start	Stop	Notes	Start	Stop	Notes	Start	Stop	Notes
716.13	716.15	t	1210.32	1210.34	t	1240.12	1240.15	x
717.70	717.72	t	1211.71	1211.73	t	1241.42	1241.44	x
722.13	722.15	t	1212.86	1212.88	t	1242.25	1242.27	x
724.57	724.59	t	1213.37	1213.39	t	1243.56	1243.59	x
726.05	726.07	x	1214.37	1214.39	t	1244.44	1244.45	x
727.62	727.64	x	1215.57	1215.59	t	1245.52	1245.53	x
730.86	730.88	x	1216.49	1216.51	t	1246.22	1246.24	x
732.56	732.59	x	1217.03	1217.05	t	1247.13	1247.15	x
733.64	733.66	x	1218.23	1218.25	t	1248.51	1248.53	x
735.63	735.64	x	1220.51	1220.53	t	1249.34	1249.36	x
738.39	738.41	x	1221.18	1221.20	t	1250.29	1250.31	x
740.40	740.41	x	1222.24	1222.25	t	1251.08	1251.10	x
742.81	742.83	x	1223.50	1223.52	t	1251.79	1251.81	x
744.41	744.43	x	1224.37	1224.39	t	1252.88	1252.89	x
746.08	746.10	x	1225.84	1225.86	t	1254.14	1254.15	x
747.48	747.50	x	1226.45	1226.47	x	1255.84	1255.86	x
748.81	748.83	x	1227.35	1227.37	x	1256.96	1256.98	x
751.90	751.92	x	1228.42	1228.44	x	1257.84	1257.86	x
753.37	753.39	x	1229.82	1229.83	x	1258.82	1258.84	x
754.99	755.02	x	1230.79	1230.81	x	1259.36	1259.38	x
757.94	757.96	x	1231.60	1231.64	x	1260.45	1260.47	x
758.90	758.93	x	1232.56	1232.58	x	1261.31	1261.33	x
759.62	759.65	x	1233.80	1233.82	x	1262.55	1262.58	x
760.71	760.74	t	1234.50	1234.53	x	1263.57	1263.59	x
761.10	761.13	t	1235.44	1235.48	x	1264.45	1264.47	x
763.65	763.67	t	1236.67	1236.70	x	1265.05	1265.07	t
765.80	765.84	t	1237.58	1237.60	x	1266.17	1266.19	t
766.67	766.71	t	1238.33	1238.35	x	1267.07	1267.09	t
768.40	768.44	t	1239.14	1239.16	x	1269.80	1269.82	t
769.07	769.10	t						

Notes: t=microwindow used to define the 100% transmittance level.

x=microwindow in the region used to measure the total absorption by N_2O_5.

TABLE 3. N_2O_5 Volume Mixing Ratio (VMR) Profiles in the Southern (Sunrise) Hemisphere Obtained May, 1985, by the ATMOS Experiment on Spacelab 3

HT km	PRES mbar	TEMP K	SR05 (47.0°S) VMR ppbv	Error(%) P	A	SR06 (46.9°S) VMR ppbv	Error(%) P	A	Weighted Average VMR ppbv	Error(%) P	A
37.5	3.7	227.7	1.31	19	28	1.34	31	38	1.32	16	26
35.5	5.0	225.5	1.52	13	24	1.56	26	34	1.53	12	23
33.5	6.7	222.4	1.62	9	22	1.65	26	34	1.63	8	22
31.5	9.1	219.1	1.59	8	22	1.62	26	34	1.60	7	21
29.5	12.5	218.7	1.43	7	21	-			1.43	7	21
27.5	16.9	217.5	1.15	7	21	-			1.15	7	21
25.5	23.2	216.6	0.73	7	21	-			0.73	7	21

HT indicates altitude; PRES, pressure; TEMP, temperature; P, precision; and A, accuracy.

TABLE 4. N_2O_5 Volume Mixing Ratio (VMR) Profile in the Northern (Sunset) Hemisphere Obtained May, 1985, by the ATMOS Experiment on Spacelab 3

HT km	PRES mbar	TEMP K	VMR ppbv	Error(%)	
				P	A
29.5	12.5	231.4	0.129	38	42
27.5	16.9	226.8	0.141	24	32
25.5	23.2	221.9	0.099	32	38

HT indicates altitude; PRES, pressure; TEMP, temperature; P, precision; and A, absolute accuracy.

Figure Captions

Figure 1. Examples of microwindow measurements in the region of the N_2O_5 1246-cm^{-1} ν_{12} band obtained from ATMOS occultation SR05 and a simulation of N_2O_5 absorption with the cross sections of Massie et al. [1985]. The measurements (upper four curves) and calculated values are shown on the same scale, but have been offset vertically for clarity. The tangent heights and corresponding tangent pressures of the measured curves (top to bottom) are 41.9 km and 1.9 mbar, 33.8 km and 6.4 mbar, 26.9 km and 18.6 mbar, and 24.0 km and 29.4 mbar. Dashed lines show the fitted 100% transmittance levels derived for the 33.8- and 26.9-km scans (see text for details). Note that microwindow measurements from SR05 spectra with tangent heights (tangent pressures) of 37.6 km (3.6 mbar) and 30.1 km (11.3 mbar) are not plotted. The calculated spectrum was computed with the room temperature N_2O_5 cross sections of Massie et al. [1985] and a N_2O_5 column amount of 6.0×10^{16} molecules cm^{-2}.

Figure 2. Comparison of measured microwindow transmittances and calculated transmittances in the region of the the 1246-cm^{-1} band of N_2O_5. The measured transmittances have been derived from an ATMOS SR05 spectrum with a tangent height of 26.9 km (tangent pressure 18.6 mbar). The calculated transmittances have been computed with the room temperature N_2O_5 cross sections of Massie et al. [1985] and a N_2O_5 column of 4.5×10^{16} molecules cm^{-2}. The spectral limits of the cross section data are 1225 to 1265 cm^{-1}.

Figure 3. Measured equivalent widths of the 1246-cm^{-1} ν_{12} N_2O_5 band as a function of tangent height derived from ATMOS sunrise occultation SR05 and the filter 2

zonal spectra. Error bars indicate the estimated two sigma error limits of the equivalent widths.

Figure 4. Comparison of microwindow measurements in the region of the N_2O_5 1246-cm^{-1} band obtained from a filter 2 zonal average spectrum (upper curve) recorded at a tangent height of 26.0 km (tangent pressure 21.8 mbar) and a SR05 spectrum (lower curve) recorded at a tangent height of 37.6 km (tangent pressure 3.6 mbar). The data from the two spectra are shown on the same scale, but have been offset vertically for clarity. Dashed lines show the fitted 100% transmittance levels derived for the scans (see text for details).

Figure 5. Sunrise (SR06) and filter 1 zonal average sunset spectra in the region of the 743-cm^{-1} band of N_2O_5. The spectra are normalized to the highest measured intensity in the plotted region, and are shown on an expanded vertical scale. The curve above the sunrise spectrum shows transmittances calculated with the N_2O_5 cross sections obtained at 273 K by Cantrell et al. [1988, Figure 1] and a N_2O_5 column amount of 2.0×10^{16} molecules cm^{-2}.

Figure 6. Examples of microwindow measurements in the region of the N_2O_5 743-cm^{-1} feature (ν_3 and ν_{14} bands) obtained from occultation SR06 spectra (upper three plots) and a simulation of N_2O_5 absorption with the cross sections of Cantrell et al. [1988, Figure 1] (bottom plot). The measured and calculated curves are shown on the same scale, but have been offset vertically for clarity. The tangent heights and corresponding tangent pressures of the measured curves (top to bottom) are 41.4 km and 2.1 mbar, 33.3 km and 6.9 mbar, and 29.8 km and 11.8 mbar. Dashed lines show the fitted 100% transmittance levels derived for

the 33.3- and 29.8-km scans (see text for details). The calculated spectrum was computed with a N_2O_5 column amount of 4.0×10^{16} molecules cm^{-2}.

Figure 7. Comparison of N_2O_5 VMR profiles retrieved from the ATMOS/SL3 observations with predawn measurements obtained by the SIRIS instrument [Kunde et al., 1988] and diurnal photochemical model predictions for the ATMOS measurement conditions. The ATMOS error bars (1 sigma) are shown at several altitudes. Models 1 and 2 denote the model calculations of M. Natarajan (private communication, 1989) and M. Allen (private communication, 1989), respectively.
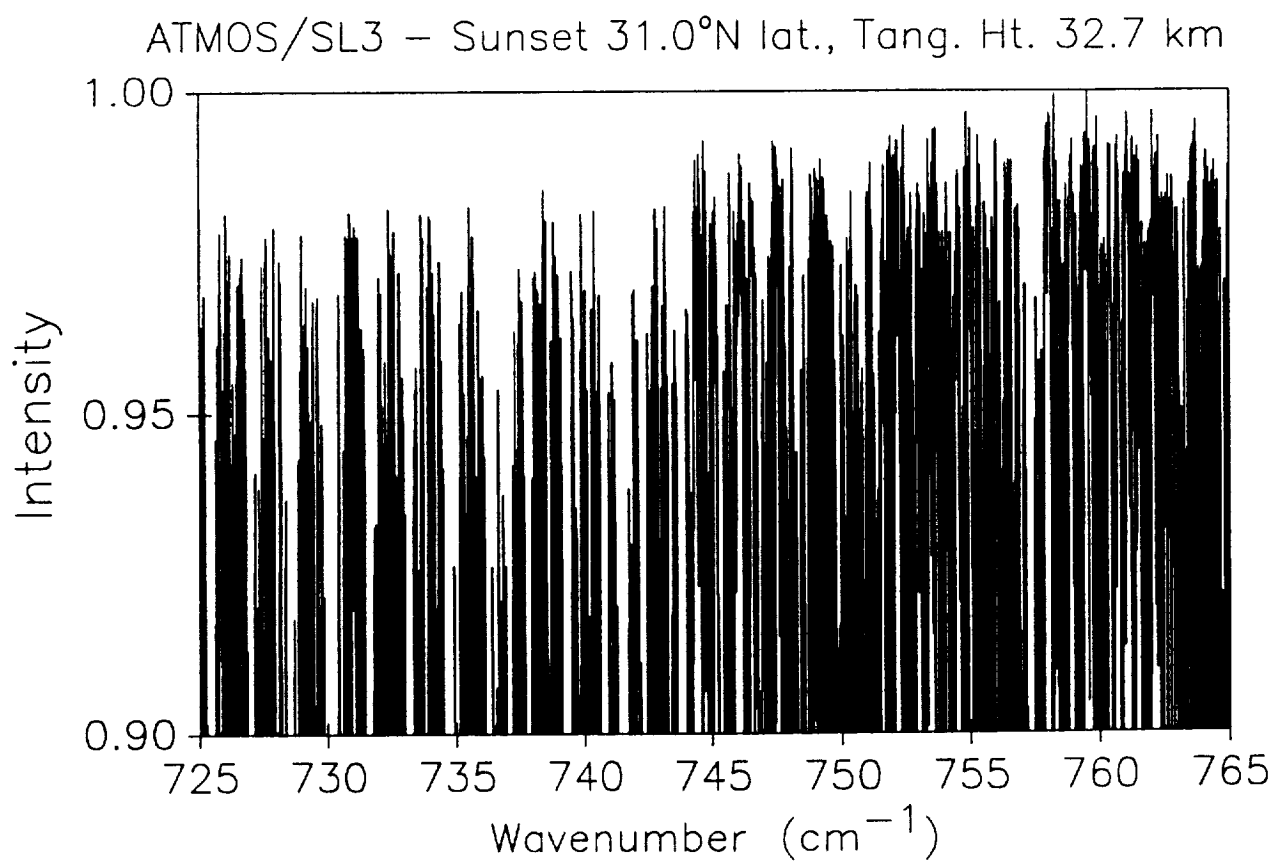
Figure 1
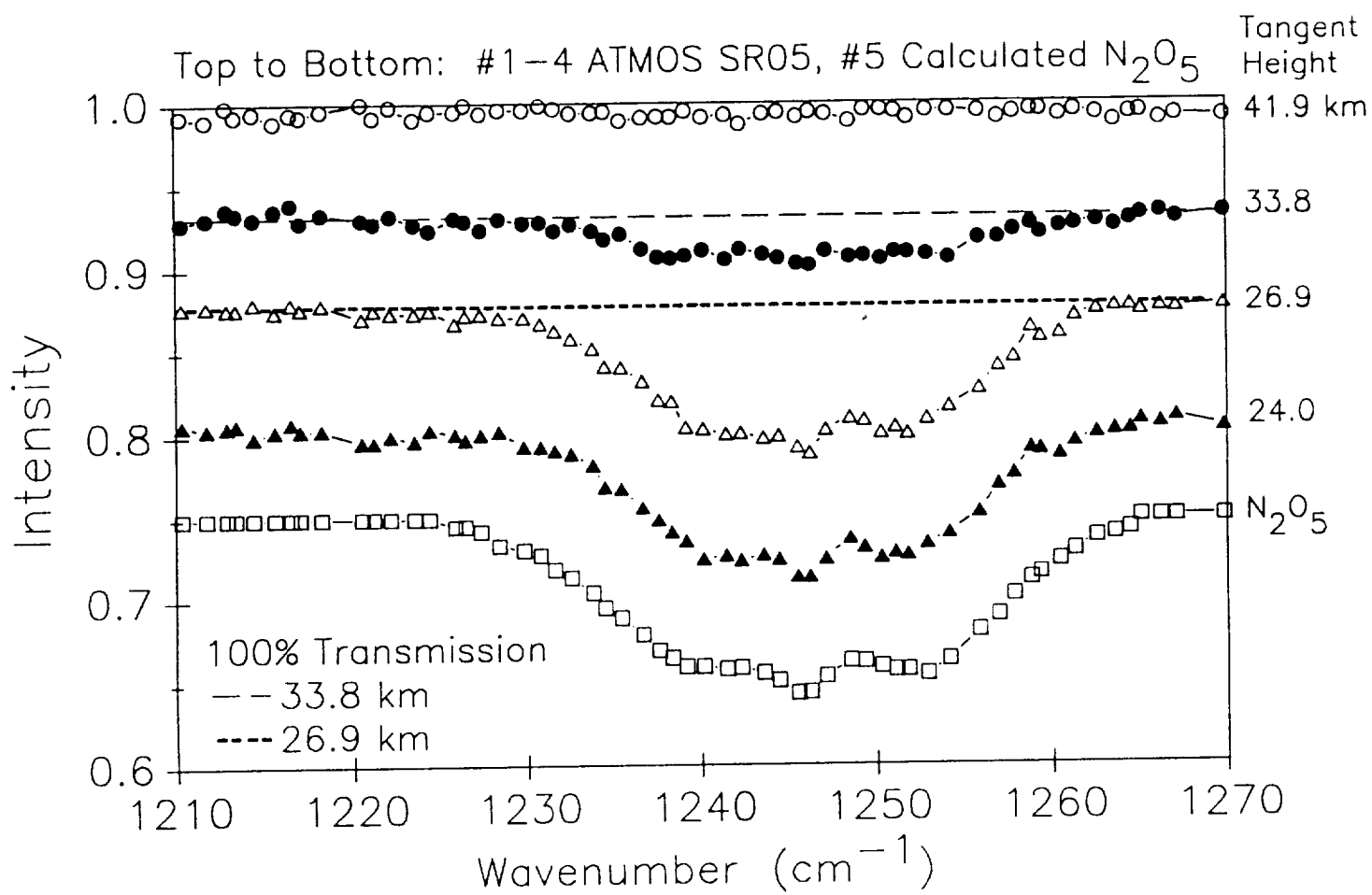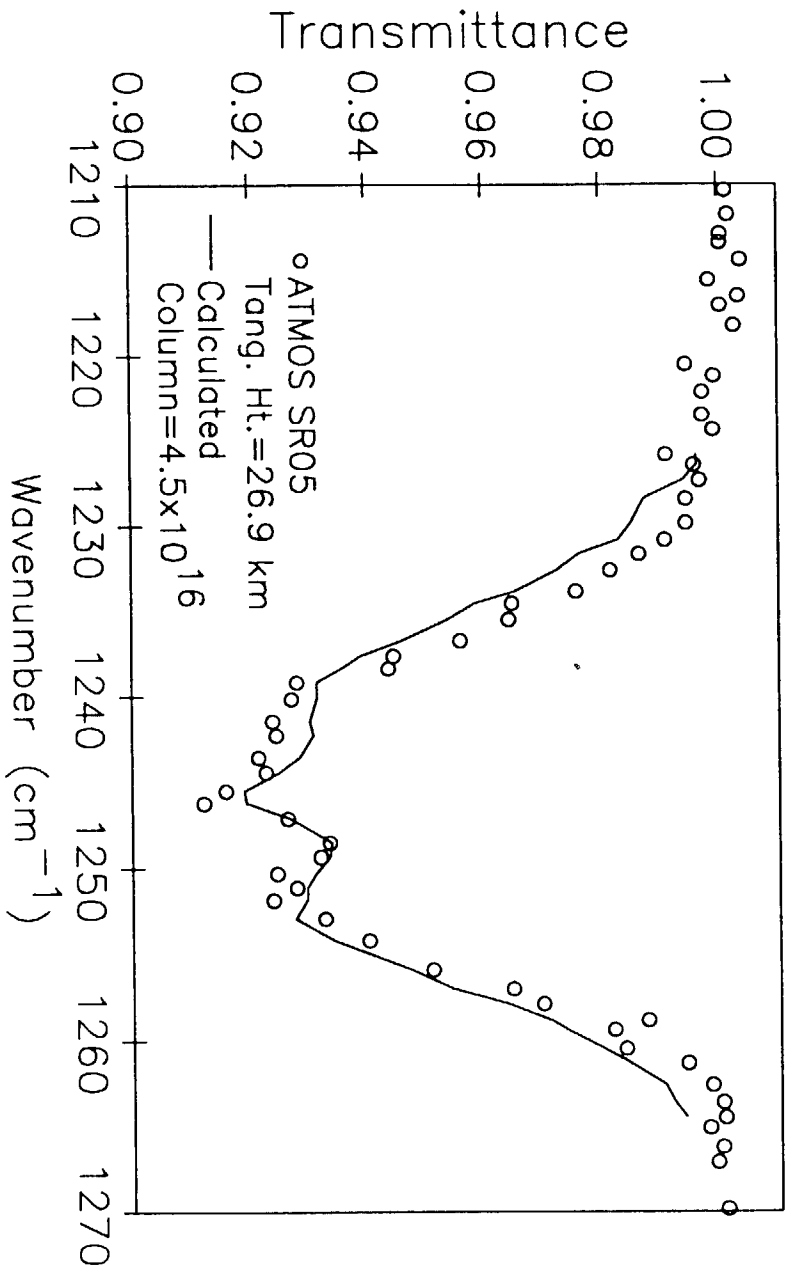
Figure 2

Figure 3

Figure 4

N$_2$O$_5$ Microwindow Measurements—ATMOS SL3

Figure 5   35

ATMOS/SL3 – Sunrise 46.9°S lat., Tang. Ht. 33.3 km

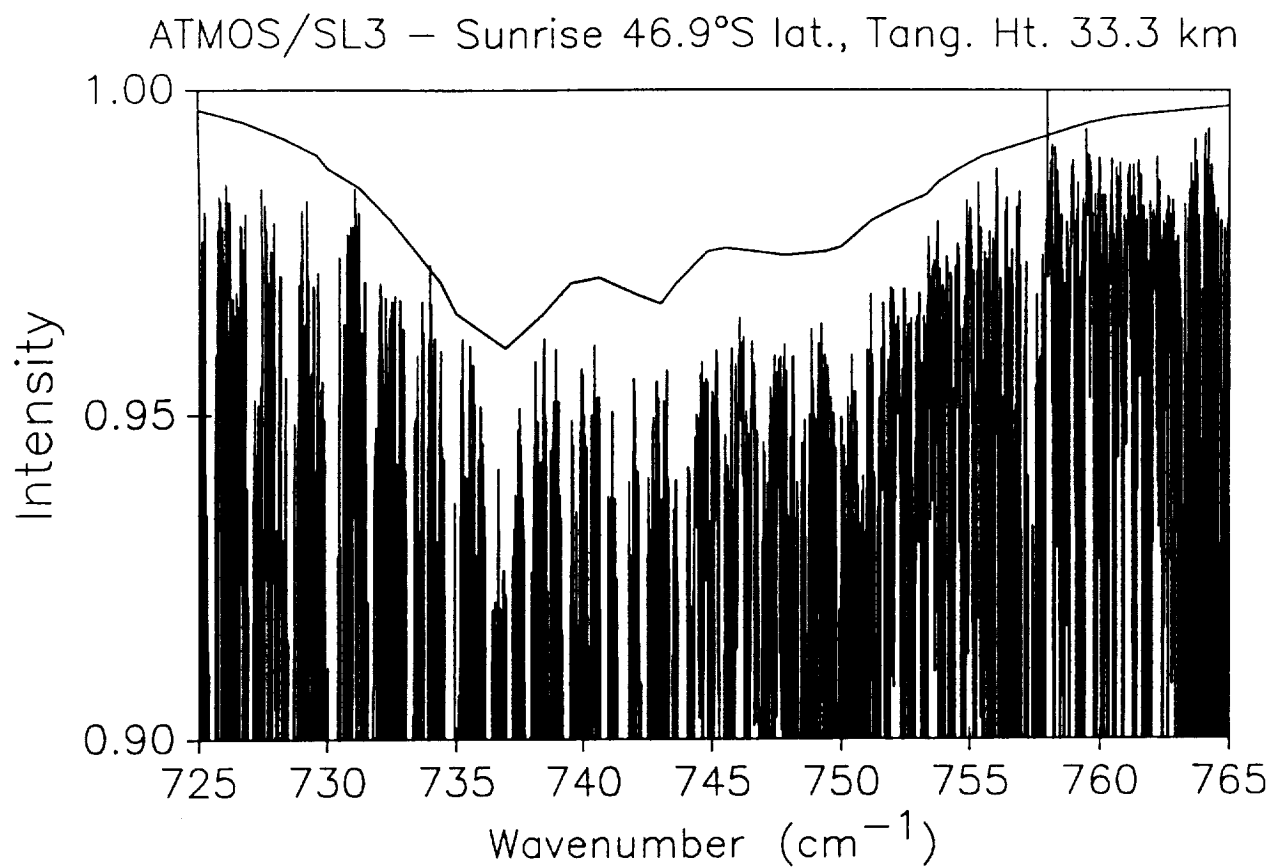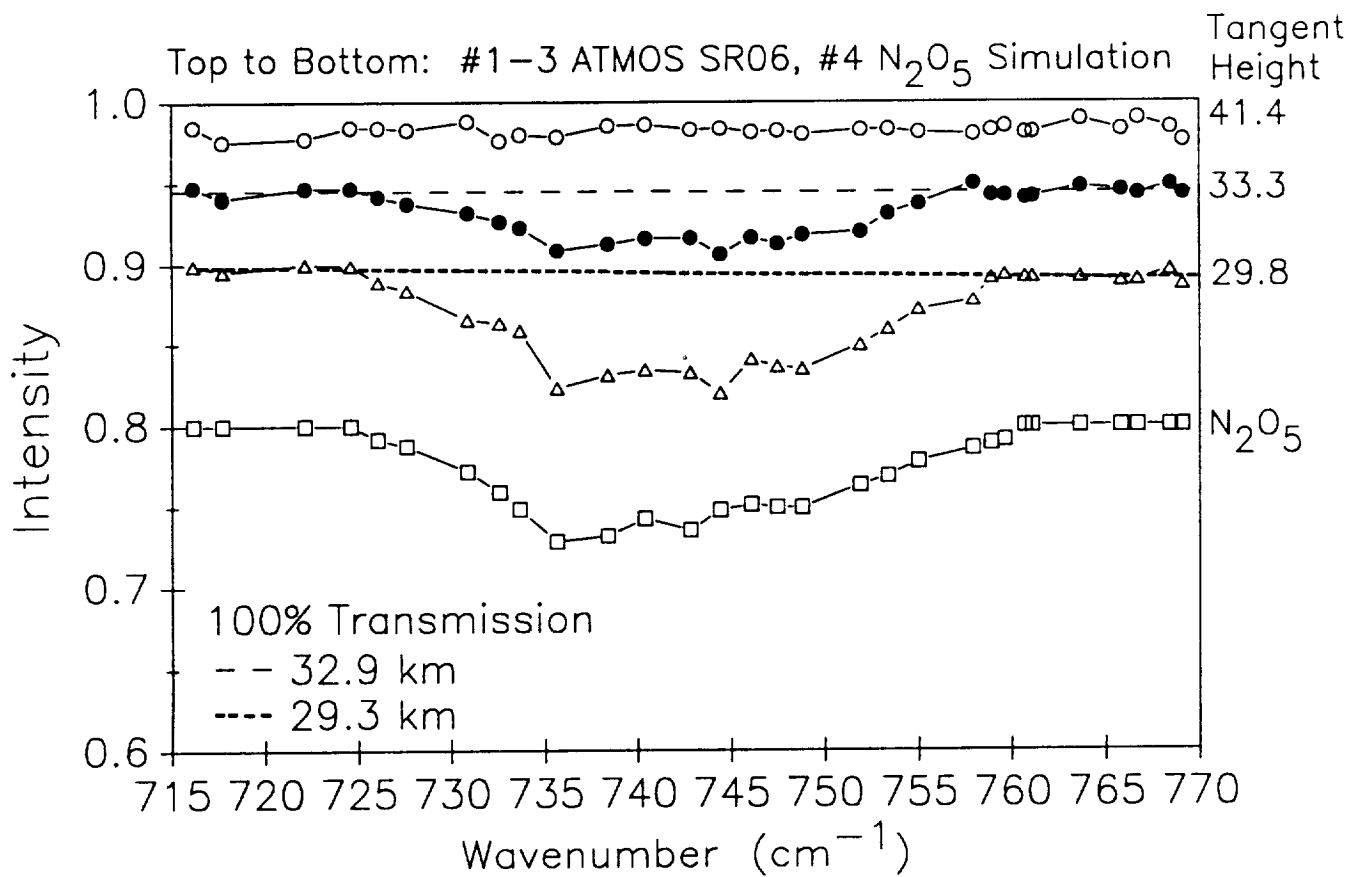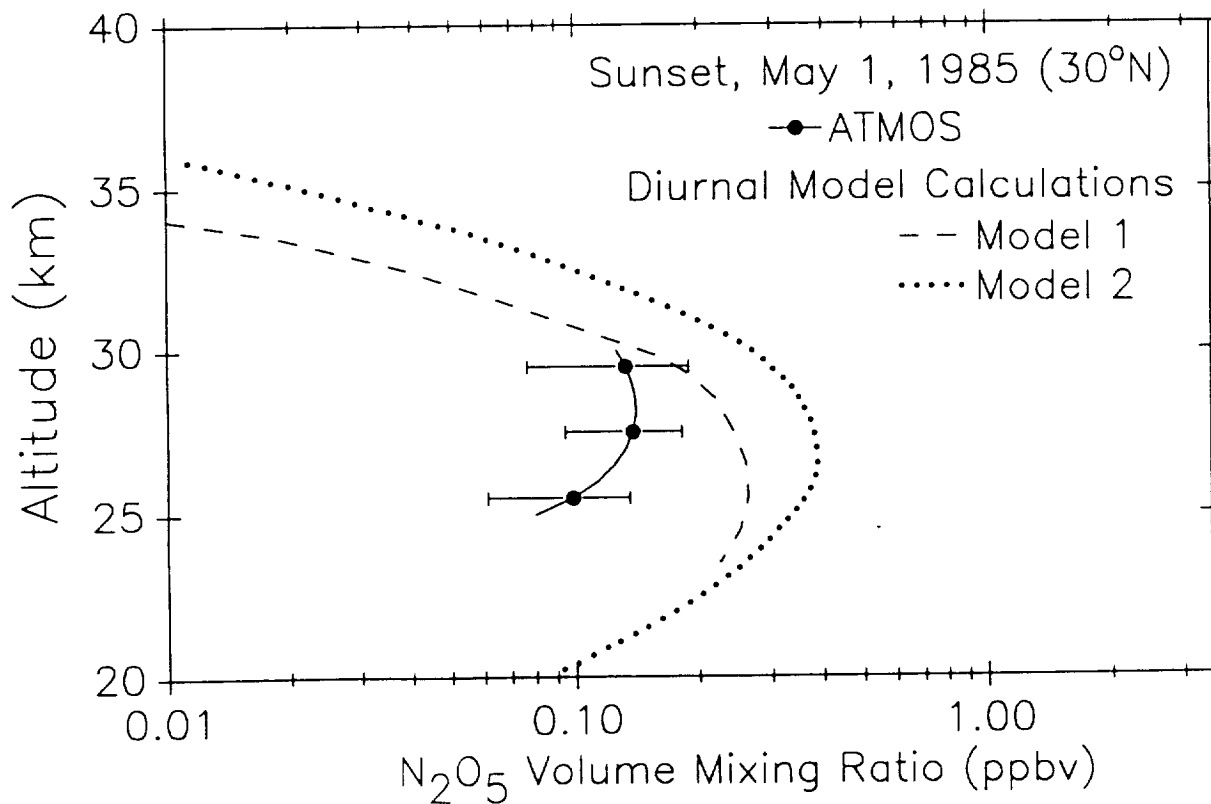ATMOS/SL3 – Sunset 31.0°N lat., Tang. Ht. 32.7 km
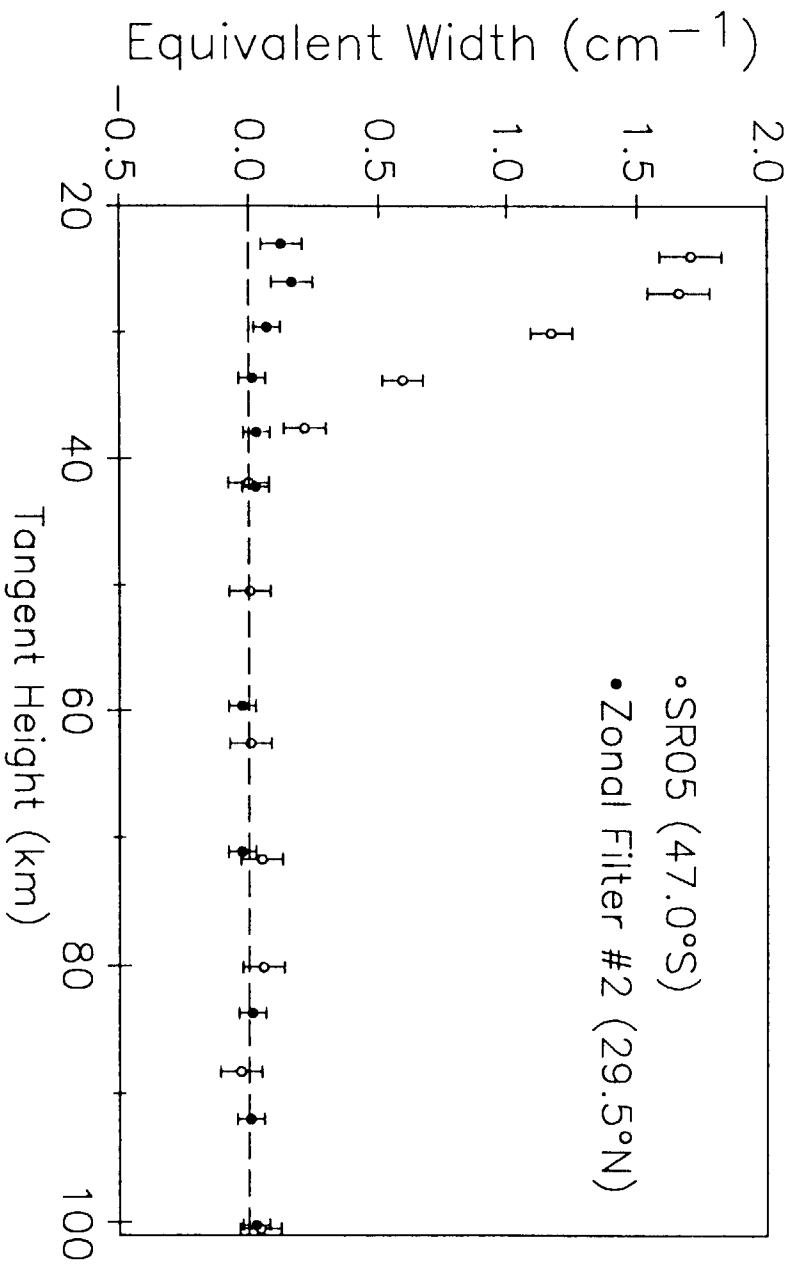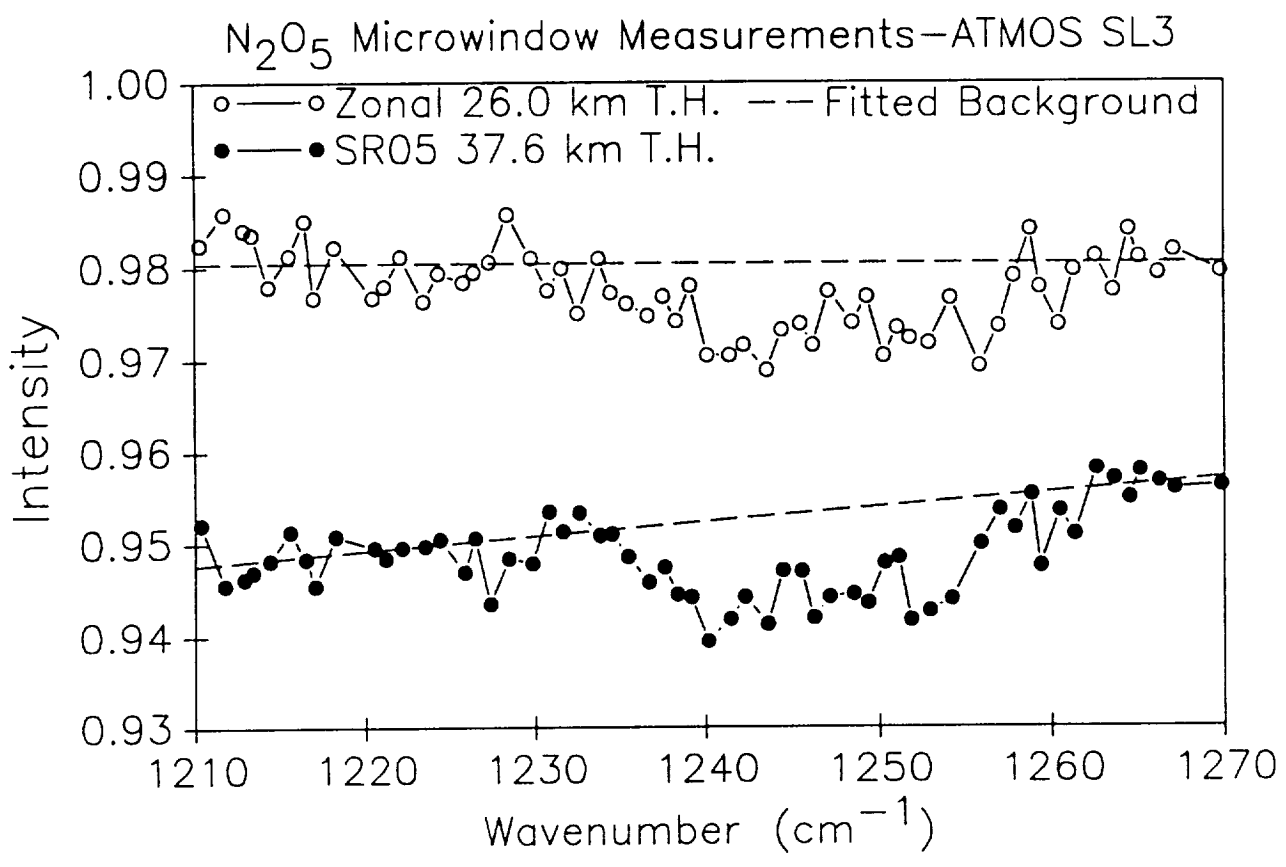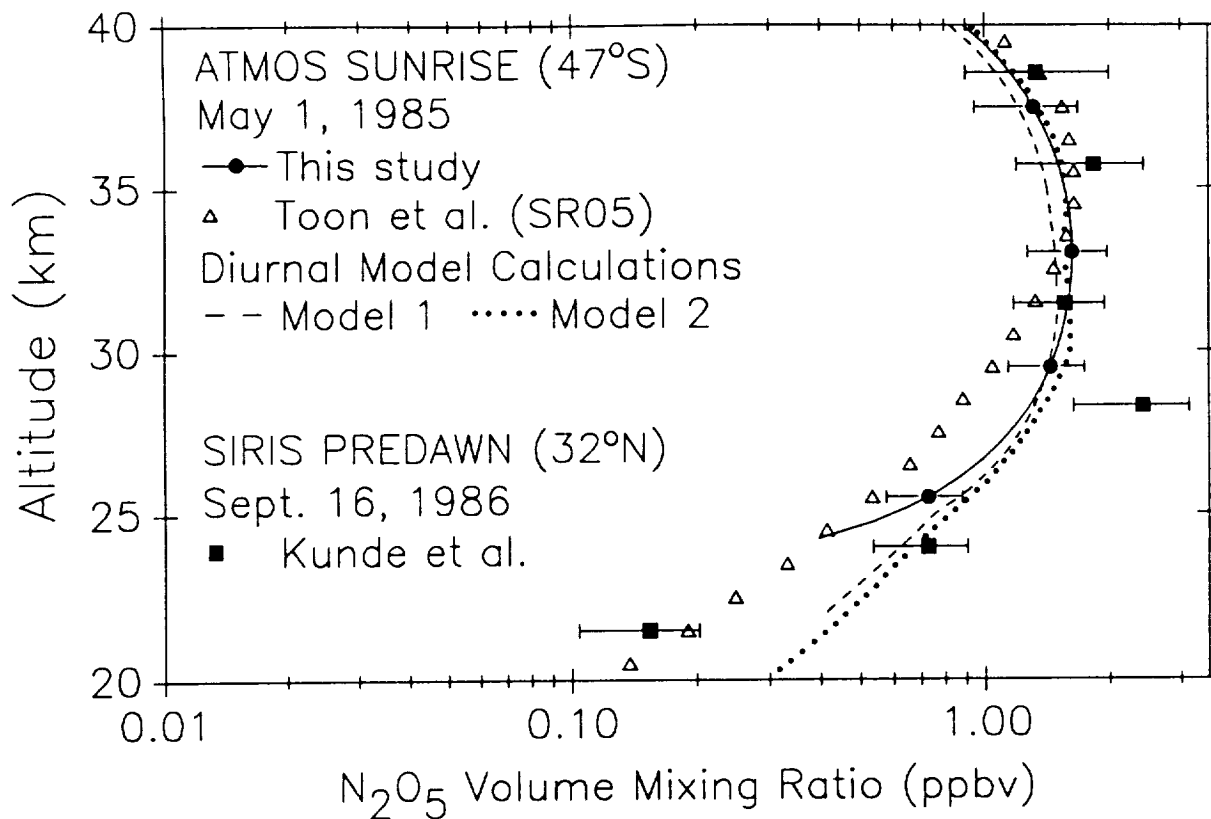
Figure 6

Figure 7

Figure 7

Mailing Addresses

G. C. Toon, C. B. Farmer, and R. H. Norton, Jet Propulsion Laboratory, California Institute of Technology, Mail Stop 183-401, 4800 Oak Grove Drive, Pasadena, CA 91109.

C. P. Rinsland, Atmospheric Sciences Division, NASA Langley Research Center, Mail Stop 401A, Hampton, VA 23665-5225.

J. S. Namkung, ST Systems Corporation, 28 Research Drive, Hampton, VA 23666.

0340 Middle atmosphere-composition and chemistry
NEW OBSERVATIONS OF STRATOSPHERIC N_2O_5

C. P. Rinsland, (NASA Langley Research Center,
Atmospheric Sciences Division, Mail Stop 401A,
Hampton, VA 23665-5225), G. C. Toon, C. B. Farmer,
R. H. Norton, J. S. Namkung

The unequivocal detection of N_2O_5 in the
stratosphere was reported by Toon et al. (1986, 1987)
based on measurements of the absorption by the N_2O_5
bands at 1246 and 1720 cm^{-1} in solar occultation
spectra recorded at sunrise near 47°S latitude by the
Atmospheric Trace Molecule Spectroscopy (ATMOS)
experiment during the Spacelab 3 (SL3) shuttle mission
(April 29 - May 6, 1985). In this work, we report
additional measurements and analysis of stratospheric
N_2O_5 derived from the ATMOS/SL3 spectra. The primary
results are the detection and measurement of N_2O_5
absorption at sunset in the lower stratosphere, the
inversion of a precise (10%) N_2O_5 sunrise vertical
distribution between 25.5- and 37.5-km altitude, and
the identification and measurement of absorption by
the N_2O_5 743-cm^{-1} band at sunrise. Assuming 4.32 x
10^{-17} and 4.36 x 10^{-17} cm^{-1}/molecule cm^{-2} respectively
for the integrated intensities of the 1246 and
743 cm^{-1} bands at stratospheric temperatures,
retrieved volume mixing ratios in parts per billion by
volume (ppbv) at sunrise (47°S latitude) are 1.32 ±
0.34 at 37.5 km, 1.53 ± 0.35 at 35.5 km, 1.63 ± 0.36
at 33.5 km, 1.60 ± 0.34 at 31.5 km, 1.43 ± 0.30 at
29.5 km, 1.15 ± 0.24 at 27.5 km, and 0.73 ± 0.15 at
25.5 km. Retrieved VMRs in ppbv at sunset (30°N
latitude) are 0.13 ± 0.05 at 29.5 km, 0.14 ± 0.05 at
27.5 km, 0.10 ± 0.04 at 25.5 km. Quoted error limits
(1 sigma) include the error in the assumed band
intensities (20%). Within the error limits of the
measurements, the inferred mixing ratios at sunrise
agree with diurnal photochemical model predictions
obtained by two groups using current photochemical
data. The measured mixing ratios at sunset are
lower than the model predictions with differences
of about a factor of 2 at 25-km altitude.

0360